Oncogene (2007), 1–9

www.nature.com/onc

ORIGINAL ARTICLE

Characterization of mammary tumors from *Brg1* heterozygous mice

SJ Bultman[1,2], JI Herschkowitz[1,2], V Godfrey[3], TC Gebuhr[1,2,5] M Yaniv[4], CM Perou[1,2] and T Magnuson[1,2]

[1]*Department of Genetics, University of North Carolina, Chapel Hill, NC, USA;* [2]*The Carolina Genome Sciences Center, University of North Carolina, Chapel Hill, NC, USA;* [3]*Department of Pathology and Laboratory Medicine, University of North Carolina, Chapel Hill, NC, USA and* [4]*Gene Expression and Disease Unit, Department of Developmental Biology, Pasteur Institute, Paris, France*

Mammalian SWI/SNF-related complexes have been implicated in cancer based on some of the subunits physically interacting with retinoblastoma (RB) and other proteins involved in carcinogenesis. Additionally, several subunits are mutated or not expressed in tumor-derived cell lines. Strong evidence for a role in tumorigenesis *in vivo*, however, has been limited to *SNF5* mutations that result primarily in malignant rhabdoid tumors (MRTs) in humans and MRTs as well as other sarcomas in mice. We previously generated a null mutation of the *Brg1* catalytic subunit in the mouse and reported that homozygotes die during embryogenesis. Here, we demonstrate that *Brg1* heterozygotes are susceptible to mammary tumors that are fundamentally different than *Snf5* tumors. First, mammary tumors are carcinomas not sarcomas. Second, $Brg1^{+/-}$ tumors arise because of haploinsufficiency rather than loss of heterozygosity. Third, $Brg1^{+/-}$ tumors exhibit genomic instability but not polyploidy based on array comparative genomic hybridization results. We monitored $Brg1^{+/-}$, $Brm^{-/-}$ double-mutant mice but did not observe any tumors resembling those from *Snf5* mutants, indicating that the $Brg1^{+/-}$ and $Snf5^{+/-}$ tumor phenotypes do not differ simply because *Brg1* has a closely related paralog whereas *Snf5* does not. These findings demonstrate that BRG1 and SNF5 are not functionally equivalent but protect against cancer in different ways. We also demonstrate that $Brg1^{+/-}$ mammary tumors have relatively heterogeneous gene expression profiles with similarities and differences compared to other mouse models of breast cancer. The $Brg1^{+/-}$ expression profiles are not particularly similar to mammary tumors from *Wap-T121* transgenic line where RB is perturbed. We were also unable to detect a genetic interaction between the $Brg1^{+/-}$ and $Rb^{+/-}$ tumor phenotypes. These latter findings do not support a BRG1–RB interaction *in vivo*.
Oncogene advance online publication, 16 July 2007; doi:10.1038/sj.onc.1210664

Keywords: BRG1; SWF/SNF; breast cancer; haploinsufficiency; genomic instability

Correspondence: Dr SJ Bultman, Department of Genetics, University of North Carolina, 103 Mason Farm Road, 4340B MBRB, Chapel Hill, NC 27599-7264, USA.
E-mail: Scott_Bultman@med.unc.edu
[5]Current address: Novartis Institutes for Biomedical Research, Cambridge, MA 02139, USA.
Received 1 May 2007; revised 7 June 2007; accepted 11 June 2007

Introduction

Much work has focused on the role of mammalian SWI/SNF-related complexes in cancer. SWI/SNF-related subunits physically interact with a number of proteins encoded by tumor-suppressor genes and proto-oncogenes (Muchardt and Yaniv, 2001; Roberts and Orkin, 2004). For example, BRM and BRG1 bind retinoblastoma (RB) and are required to repress the activity of E2F1, inhibit the transcription of cyclins A and E and mediate G_1 cell-cycle arrest *in vitro*. BRG1 and SNF5 can also act upstream of RB by activating the expression of several cyclin-dependent kinase inhibitors ($p15^{INK4b}$, $p16^{INK4A}$ or $p21^{CIP1/WAF1}$), which leads to the inhibition of CDK2 and CDK4 and accumulation of the hypophosphorylated form of RB that mediates G_1 arrest.

In addition to being associated with cancer-related proteins, the BRM, BRG1, SNF5, BAF155 and BAF250 subunits are mutated or not expressed in various tumor-derived cell lines (Muchardt and Yaniv, 2001). When tumor-derived cell lines are cultured, however, deletions and epigenetic alterations are selected for and accumulate. Because of this caveat, it is crucial to identify and characterize mutations in primary tumors to confirm they are functionally important and not merely a secondary consequence of prolonged cell culture. *BRG1* mutations have been identified in primary lung tumors (Medina *et al*., 2004). Although these mutations are not common, 10% of primary lung tumors analysed in another study lacked expression of both BRM and BRG1 (Reisman *et al*., 2003). The evidence is more compelling for *SNF5*, which is a bona fide tumor-suppressor gene that undergoes loss of heterozygosity (LOH) in malignant rhabdoid tumors (MRTs) as well as choroid plexus and possibly other tumors (Roberts and Orkin, 2004).

Snf5 mouse models have recapitulated and extended the findings from human patients. *Snf5* null heterozygous mice (15–30%) develop MRTs or other sarcomas with a median latency period of 12 months (reviewed in Roberts and Orkin, 2004). The LOH, histopathological features, polyploidy, ability to metastasize and expression profiles of some mouse tumors are similar to human tumors (Roberts and Orkin, 2004; Isakoff *et al*., 2005).

We previously generated a *Brg1* (*Smarca4*) null mutation in the mouse and reported that homozygotes

die embryonic development (Bultman *et al*., 2000). We also presented preliminary evidence that heterozygotes are tumor prone but were unable to distinguish whether these tumors were of apocrine or mammary gland origin because of the small number of tumors and limited analysis. Here, we present a detailed characterization of the *Brg1*$^{+/-}$ tumor phenotype. In contrast to *Snf5* heterozygotes, *Brg1* heterozygotes are susceptible to mammary tumors that arise because of haploinsufficiency and exhibit genomic instability but not polyploidy. Rather than protecting against tumorigenesis in a simple manner, SWI/SNF-related complexes utilize different subunits and strategies in unrelated tissues.

Results

Penetrance, latency and histopathology of Brg1$^{+/-}$ *tumors*

We monitored 130 *Brg1* null heterozygous mice and 100 wild-type siblings as controls for at least 18 months under identical conditions without any exposure to ionizing radiation (IR) or carcinogens. A total of 12/130 heterozygotes developed macroscopic tumors, corresponding to a penetrance of 9.2%. The latency period ranged from 7 to 19 months with a median of 14 months (Table 1). Although 10/12 tumor-bearing animals were females, more heterozygous females ($n=85$) were aged than males ($n=45$). As a result, the penetrance among females (11.8%) compared to males (4.4%) did not reach statistical significance ($0.10<P<0.25$). We did not detect macroscopic tumors in any of the 100 wild-type controls.

All 12 tumors were subcutaneous and located along the ventral or ventral-lateral surface of the mice from the neck to the inguinal region, which suggested they were mammary tumors. Analysis of hematoxylin and eosin (H&E)-stained tumor sections from the 10 females confirmed each one was a mammary adenocarcinoma or carcinoma (Table 1). All 10 tumors were malignant and shared a number of histopathological characteristics. For example, the predominant cell type in each tumor was a nondescript, polyhedral-shaped epithelial cell growing in cords, and the nuclear:cytoplasmic ratio was high compared to normal mammary epithelial tissue (Figure 1a). The nuclei did not have a basal orientation and contained finely clumped chromatin with relatively few nucleoli (Figure 1a). The number of mitotic figures was modest for a tumor, ranging from 1 to 10 per high-powered field. Tumor cells were present inside blood vessels (that is, tumor emboli), which suggests metastatic potential although no macroscopic metastases were observed (Figure 1b). However, these tumors also exhibited histopathological differences. For example, some had trabecular or papillary features, whereas others were squamous. Table 1 provides a brief description of each tumor. One of the two male tumors was also a mammary adenocarcinoma, whereas the other was an osteosarcoma (Table 1). We did not observe any MRTs or other types of tumors in *Brg1* heterozygous mice.

Brg1$^{+/-}$ *tumors have heterogeneous gene expression profiles with similarities and differences to mammary tumors from other mouse models of breast cancer*

To support and extend our histopathological findings, we performed gene-expression profiling on *Brg1*$^{+/-}$ tumors and compared their profiles to each other as well as normal mammary tissue and mammary tumors from other mouse models of breast cancer (Figure 2a, Supplementary Table S2). This comparison was facilitated by our previous analysis of gene-expression profiles from 10 normal mammary glands and 108 unique mammary tumors from 13 distinct mouse models (Herschkowitz *et al*., 2007). *Brg1*$^{+/-}$ tumors 172 and 284 were tightly clustered to each other as well as *MMTV-Neu* and *MMTV-PyMT* mammary tumors (Figure 2a, Table 1). Based on their expression profiles, these

Table 1 Tumors from *Brg1* heterozygous mice

Number	*Gender*	*Latency*[a]	*H&E description*	*Expression profile group*	*Cytokeratin expression*		
					K8/18	*K5*	*K14*
172	F	12	Trabecular/papillary mammary adenocarcinoma	A	+	–	ND
284	M	14	Trabecular/papillary mammary adenocarcinoma	A	+	–	–
135	F	7	Mammary adenocarcinoma with squamous metaplasia	B	+	+	ND
2023	F	15	Mammary adenocarcinoma with extensive squamous metaplasia	B	+	+	+
55	F	16	Trabecular mammary adenocarcinoma with necrosis	C	+	+/–	+
160	F	14	Trabecular mammary carcinoma with extensive necrosis	C	+	+/–	+
2134	F	19	Mammary adenocarcinoma with mild squamous metaplasia	C	+	+	+
920	F	12	Trabecular/papillary mammary adenocarcinoma[b]	D	+	+	+
221	F	17	Well-differentiated squamous cell mammary carcinoma	E	+	+	ND
372	F	14	Mammary adenocarcinoma with extensive squamous metaplasia	E	+	+	+
646	F	18	Infiltrative mammary carcinoma of small cuboidal cells	F	+	–	–
1766	M	12	Subcutaneous osteosarcoma	G	–	–	–

Abbreviations: A, clusters with mammary tumors from *MMTV-Neu* and *MMTV-PyMT* mice; B, clusters with mammary tumors from two *Brca1* mutants and *MMTV-Wnt1* mice; C, clusters with mammary tumors from *Wap-T121* mice; D, clusters relatively close to tumors 55, 160 and 2134 in group C; E, clusters with DMBA-induced squamous mammary tumors; F, unique; G, unique but similar to DMBA-induced spindloid tumors; H&E, hematoxylin and eosin; ND, not determined; +/–, few positive cells. [a]Age in months that tumor reached end-stage status (1–2 cm). [b]More cytologically aggressive than tumors 172 and 284.

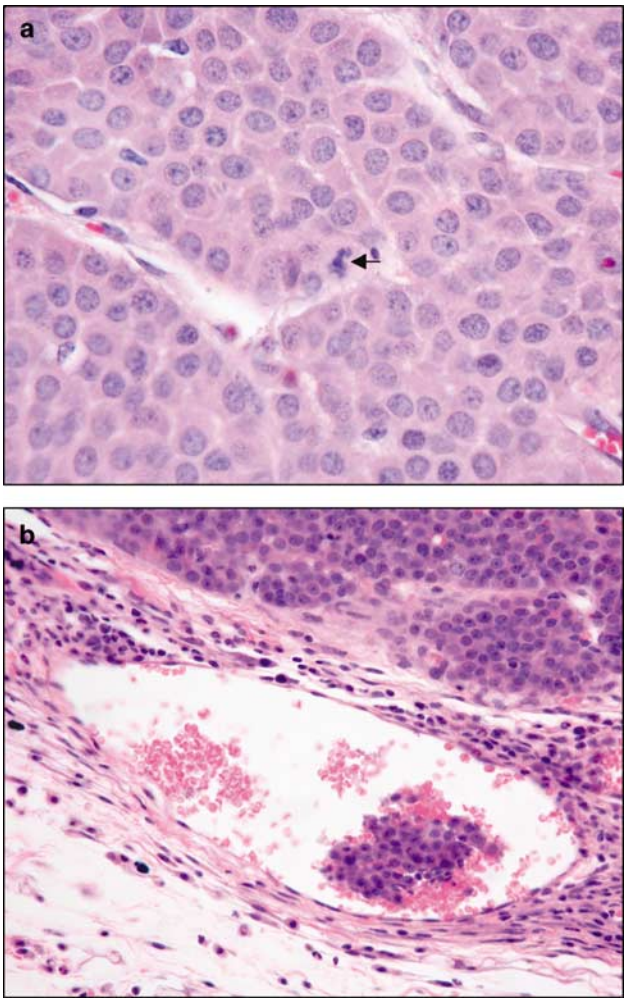

Figure 1 Histopathology of $Brg1^{+/-}$ tumors. (**a**) Representative image of tumor cells in an H&E-stained tumor section at $\times 800$ magnification. The section is predominated by nondescript, polyhedral-shaped tumor cells with a relatively high nuclear/cytoplasmic ratio. The nuclei are not oriented basally and have finely clumped chromatin. A mitotic figure is indicated with an arrow. (**b**) Representative image of tumor emboli from an H&E-stained tumor section at $\times 400$ magnification. Tumor cells and red blood cells are visible inside a blood vessel lined with normal vascular endothelial cells.

tumors appear to be derived from the luminal lineage of the mammary gland and therefore have been shown to express cytokeratins (K) 8/18 but not K5 or K14. We verified that tumors 172 and 284 were positive for K8/18 but negative for K5 and K14 by immunostaining (Figure 2b, Table 1).

The expression profiles of tumors 135 and 2023 were tightly clustered to each other and mammary tumors from two different *Brca1*-deficient models and *MMTV-Wnt1* transgenic mice (Figure 2a, Table 1). Tumors with these expression profiles are known to express K8/18 and K5 or K14 in nonoverlapping areas suggesting that they are derived from mammary progenitor cells that differentiate into both the luminal and basal/myoepithelial lineages. We verified that tumors 135 and 2023 express K8/18 and K5 or K14 in distinct areas (Figure 2c, Table 1).

Tumors 55, 160 and 2134 had expression profiles that clustered with each other and a subset of *Wap-T121* mammary tumors and to a lesser extent *Brg1* tumor 920 (Figure 2a, Table 1). Tumors 221 and 372, which exhibit squamous metaplasia based on H&E analysis, had expression profiles that clustered with each other and squamous mammary tumors from 7,12-dimethylbenz[α]anthracene-treated mice (Figure 2a, Table 1). Tumor 646 had a unique appearance by H&E and also had a unique gene-expression profile (Figure 2a, Table 1). Finally, the 1 tumor (1766) that was not scored as a mammary tumor by H&E analysis also had a unique gene-expression profile and did not express any of the cytokeratins as expected (Figure 2a, Table 1).

In addition to being used to categorize $Brg1^{+/-}$ tumors, the gene-expression profiling demonstrated that *Brg1* transcription was reduced in $Brg1^{+/-}$ tumors compared to normal mammary glands and mammary tumors from the other mouse models of breast cancer as expected (Supplementary Table S1, line 556). The gene-expression profiling also revealed numerous potential downstream targets that were upregulated or downregulated in $Brg1^{+/-}$ tumors (Supplementary Table S1). Expression Analysis Systematic Explorer was used to identify biological themes from the upregulated and downregulated gene lists. It did not identify gene ontology categories that were significantly overrepresented among the 207 upregulated genes but did indicate that genes involved in chromatin structure were overrepresented among the 469 downregulated genes (Supplementary Table S2). Bonferroni-corrected enrichment scores were highest for chromatin (7.22E-03), chromatin assembly/disassembly (2.92E-03), chromosome organization/biogenesis (1.93E-03) and nucleosome assembly (1.39E-03) among the various biological categories (Supplementary Table S2).

The Brg1 *mutation does not exacerbate the* $Rb^{+/-}$ *tumor phenotype*

BRG1 binds to hypophosphorylated RB and helps it mediate G_1 cell-cycle arrest *in vitro*. Therefore, it was surprising that the histopathology and expression profiles of the $Brg1^{+/-}$ mammary tumors were not more similar to *Wap-T121* mammary tumors where the function of RB and the other two pocket proteins (p107 and p130) are perturbed (Simin *et al*., 2004). To investigate whether *Brg1* and *Rb* genetically interact *in vivo*, we introduced the *Brg1* null mutation onto an *Rb* mutant background. *Rb* null homozygotes die during embryogenesis at mid gestation, whereas heterozygotes are viable but acquire pituitary tumors and die at around 1 year of age. We monitored 10 $Rb^{+/-}$ mice and 10 $Brg1^{+/-}$, $Rb^{+/-}$ without any exposure to IR or carcinogens. Both groups of mice acquired pituitary tumors that led to wasting and death by 14 months of age, and there was not a significant difference in the penetrance (100%) or the latency period (median age of 12–13 months) (Figure 3). All mice succumbed to *Rb*

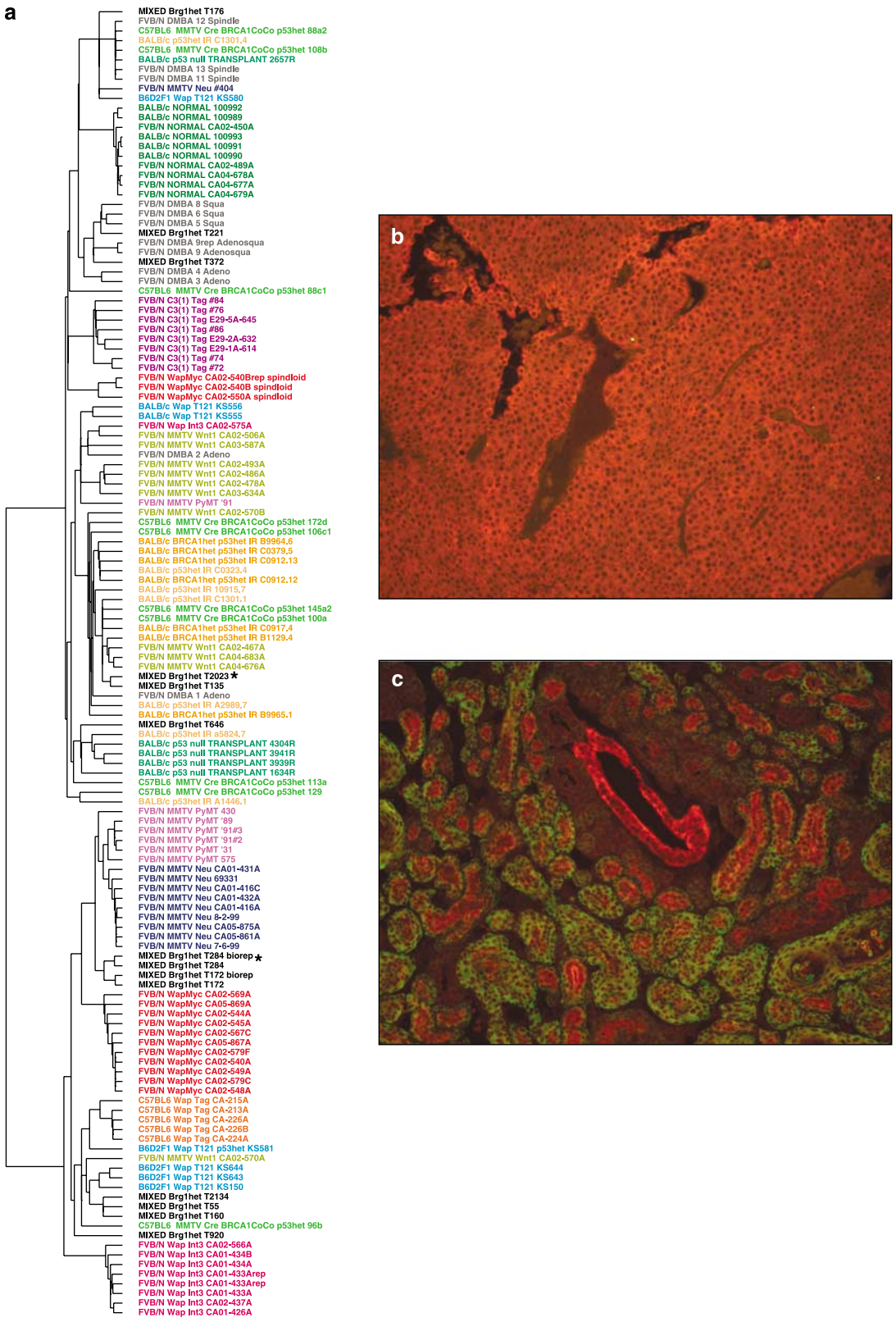

Figure 2 Characterization of *Brg1*$^{+/-}$ tumors by expression profiling and cytokeratin immunostaining. (**a**) Hierarchal clustering of gene-expression profiles showing the relationship of *Brg1*$^{+/-}$ mammary tumors with each other and with normal mammary tissue as well as mammary tumors from other mouse models of breast cancer. The 12 *Brg1* tumors are shown in black including two biological replicates. The two tumors highlighted with an asterisk are shown in (**b**) and (**c**). Normal mammary tissue from five FVB/N and five BALB/c mice are shown in dark green as a single group toward the left. Tumors from the various mouse models of breast cancer are shown in different colors. (**b** and **c**) Representative images at $\times 200$ magnification showing expression of cytokeratins (K) 8/18 (red) and K14 (green) in tumor 284 (**b**) and tumor 2023 (**c**).

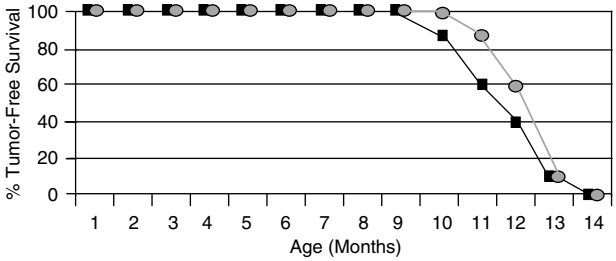

Figure 3 Kaplan–Meier survival curve of 10 *Rb* heterozygous mice (black squares) and 10 *Rb-Brg1* double-heterozygous mice (gray circles) over the course of 14 months.

pituitary tumors before *Brg1* mammary tumors or any other type of macroscopic tumor could be identified. Although the *Brg1* mutation did not exacerbate the $Rb^{+/-}$ tumor phenotype, a BRG1–RB interaction cannot be ruled out. p107 or p130 might have compensated for loss of RB, and it is also possible that the relatively early onset of *Rb*-associated lethality precluded a BRG1–RB interaction from being observed in older mice.

Brg1$^{+/-}$ *tumors do not undergo LOH but arise because of haploinsufficiency*

We genotyped all 12 $Brg1^{+/-}$ tumors for the targeted null mutation and identified each one as $+/-$ (Figure 4a, data not shown). We also performed laser-capture microdissection and genotyped pure populations of tumor cells as $+/-$ (Figure 4a). These results ruled out the possibility of a gene-conversion event or a chromosome loss-and-reduplication event (resulting in the wild-type chromosome 9 being replaced by the chromosome 9 homologue carrying the *Brg1* null allele) but did not address whether a somatically acquired mutation might have occurred in a part of the gene other than the site of the targeted mutation. Therefore, we performed reverse transcription (RT)–PCR to amplify the *Brg1* cDNA from five tumors (135, 172, 221, 284 and 920) and sequenced the entire open reading frame from each one. No deletions, splicing defects or point mutations were identified in any of the tumors.

The second hit in many tumor-suppressor genes is not a mutation but epigenetic silencing of the wild-type allele. To investigate whether the wild-type *Brg1* allele is expressed or silenced in tumor cells, we performed western blot analyses and detected robust levels of BRG1 in each case (Figure 4b). Although this result strongly suggested that the tumor cells were expressing BRG1, it was possible that all of the protein was expressed from stromal or blood cells. Utilizing a riboprobe that hybridizes to a portion of the *Brg1* 3′ untranslated region that does not share significant sequence homology to *Brm* or any other gene in the mouse genome, we detected *Brg1* mRNA throughout the tumor sections including the tumor cells (Figure 4c). In contrast, hybridization of tumor sections with a sense riboprobe as a negative control resulted in low-level

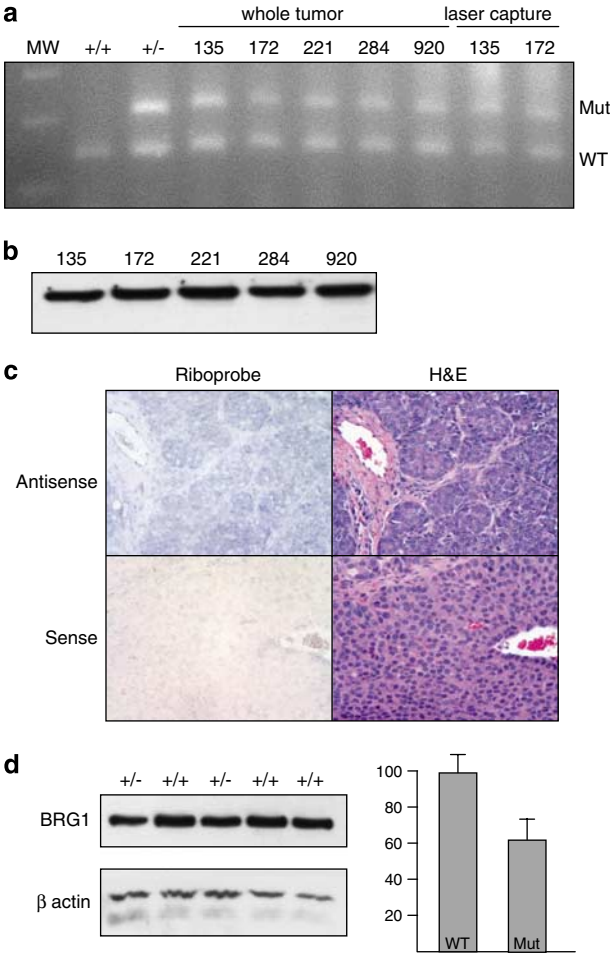

Figure 4 $Brg1^{+/-}$ tumors do not undergo LOH but arise because of haploinsufficiency. (**a**) Genotyping DNA from wild-type ($+/+$) and heterozygous ($+/-$) tails as controls plus whole tumor and laser-captured tumor samples for the *Brg1*-targeted null mutation. An image of an ethidium bromide-stained agarose gel with a molecular weight (MW) standard (100-, 200- and 300-bp fragments are visible) followed by each of the samples is shown. Wild-type (WT) and mutant (Mut) PCR products are indicated. (**b**) Western blot showing expression of BRG1 protein in $Brg1^{+/-}$ tumors. (**c**) Expression of *Brg1* mRNA in tumor cells detected by *in situ* hybridization. $Brg1^{+/-}$ tumor sections hybridized with a *Brg1* antisense riboprobe (upper left panel) and a *Brg1* sense riboprobe as a negative control (lower left panel) are shown. Adjacent hematoxylin and eosin (H&E) sections are shown to the right. (**d**) Reduced expression of BRG1 in heterozygous tissues compared to wild-type tissues. Left: a western blot of $+/+$ and $+/-$ lysates probed with BRG1 (upper) and β-actin (lower) antibodies. Right: quantification of BRG1 protein levels based on densitometry utilizing β-actin as an internal loading control.

background (Figure 4c). We also developed an RT–PCR assay that distinguishes wild-type and mutant mRNAs and detected the wild-type mRNA at the same level in $+/-$ tumors as $+/-$ control tissues (Supplementary Figure S1). These results rule out the possibility that CpG methylation or another epigenetic event silences expression of the wild-type allele in tumor cells. Taken together, the above findings indicate that *Brg1* haploinsufficiency, not LOH, underlies tumorigenesis.

Considering that *Brg1* haploinsufficiency is the mode of tumorigenesis, BRG1 should be reduced in heterozygous tissues compared to wild-type tissues. By performing western blots on heterozygous and wild-type tissues and quantifying the signal intensities by densitometry, we determined that heterozygotes express BRG1 protein at approximately 60% of wild-type levels (Figure 4d). This result is supported by gene-expression profiling data from our microarray experiments showing that *Brg1* heterozygous tumors express *Brg1* mRNA at 60% compared to normal mammary tissue and unrelated mammary tumors, which are $Brg1^{+/+}$ (see line 556 of Supplementary Table S2 showing a 0.596-fold change).

Brg1$^{+/-}$ *tumors exhibit genomic instability*

The incomplete penetrance and relatively long latency period of the tumor phenotype suggested that other genetic changes in addition to *Brg1* haploinsufficiency occur during tumorigenesis. Therefore, we compared tumor DNA to kidney DNA from three mice using array comparative genomic hybridization (CGH) analysis. We did not observe DNA copy-number gains (that is, duplications or amplifications) or losses (that is, deletions) at the *Brg1* locus (chr9:21.6 Mb) in any of the tumors, which supports our previous conclusion that LOH does not occur. However, each tumor exhibited DNA copy-number changes of various chromosomal segments, and five of these alterations were present in each tumor (Figure 5): gain of chr2:129 Mb (Figure 5a), loss of chr2:177 Mb (Figure 5a), and gains of chr4:95Mb (Figure 5b), chr15:35 Mb (Figure 5c) and chr19:38 Mb (Figure 5d). Each of the four chromosomal segments with copy-number gains had log 2 ratios >0.5 for each tumor, and the one chromosomal segment with a copy-number loss had log 2 ratios <-0.5 for two of the tumors and <-0.25 for the third. We identified 12 other copy-number changes with log2 ratios >0.25 or <-0.25 in two of the three tumors (Supplementary Table S2). Several of the chromosomal segments with copy-number changes include candidate genes that might have contributed to the initiation or progression of tumorigenesis (Supplementary Table S3).

In addition to focal aberrations affecting chromosomal segments up to $\sim$1 Mb, as described above, one of the tumors (284) had a larger $\sim$60 Mb gain of proximal chromosome 4 and whole-chromosomal gains for chromosomes 2 and 15 (Figure 5). Based on the chromosome profiles of all three tumors (Figures 5a and c), the whole-chromosomal gains (that is, trisomies) most likely occurred after the focal gains and losses described above.

Brg1$^{+/-}$, Brm$^{-/-}$ *tumors are also different than* Snf5 *tumors*

Brg1 and *Brm* are 75% identical at the amino-acid level, are both expressed in a widespread manner and have similar or identical activities in a number of *in vitro* assays. To determine whether there is functional compensation, we introduced the *Brg1* null mutation onto a *Brm*-deficient background. We monitored 20 $Brg1^{+/-}$, $Brm^{-/-}$ double-mutant mice for 16 months without any exposure to IR or carcinogens. Two of these mice displayed large subcutaneous tumors along the ventral-lateral surface of their bodies. One was a 14-month-old female with a mammary tumor, as observed for *Brg1* heterozygotes on a wild-type background, whereas the other was a 16-month-old male with a hemangiosarcoma based on analysis of H&E-stained sections. We identified numerous vascular channels in the hemangiosarcoma that varied in size (Supplementary Figure S2). These vascular channels are formed and lined by tumor cells, and the tumor cells exhibit nuclear pleiomorphism, which is typical for hemangiosarcomas (Supplementary Figure S2). The ability of *Brm* to functionally compensate for *Brg1* haploinsufficiency in the vasculature is consistent with their developmental expression because BRM is expressed specifically in the vasculature of the early postimplantation embryo, whereas BRG1 is expressed in both the vasculature and surrounding tissues (Dauvillier *et al*., 2001). Additionally, SWI/SNF-related complexes may play a particularly important role in the vasculature since two of the subunits (BAF180 and BAF60c) are required for cardiovascular development (Lickert *et al*., 2004; Wang *et al*., 2004). We did not identify any MRTs or any other type of macroscopic tumor in this experiment. Therefore, loss of *Brm* did not alter the overall penetrance of the $Brg1^{+/-}$ tumor phenotype but may have expanded the tumor spectrum. However, it will be necessary to age a larger number of $Brg1^{+/-}$, $Brm^{-/-}$ mice to determine more accurately the tumor penetrance and spectrum.

Discussion

Mammalian SWI/SNF-related complexes utilize either BRG1 or BRM as a catalytic subunit, and BRG1 is essential for viability in mice, whereas BRM is dispensable. Here, we identify important functional differences between BRG1 and SNF5 in cancer. We demonstrate that *Brg1* null heterozygotes are predisposed to mammary tumors that arise because of haploinsufficiency and genomic instability, whereas it has been shown previously that *Snf5* null heterozygotes are predisposed to MRTs and other sarcomas that undergo LOH and polyploidy. These differences are surprising because BRG1 and SNF5 are core subunits that function together in the same complexes and are required for embryonic development. The different tumor phenotypes are probably not due to functional compensation of *Brg1* haploinsufficiency by *Brm* because $Brg1^{+/-}$, $Brm^{-/-}$ double-mutant mice do not develop MRTs or other tumors observed in *Snf5* heterozygotes. It has been demonstrated that SNF5 is not required for assembly of mammalian SWI/SNF-related complexes or BRG1-dependent functions *in vitro* (Doan *et al*., 2004), suggesting that *Brg1* and *Snf5* mutant complexes are stable but compromised in different ways. However, the molecular basis of these

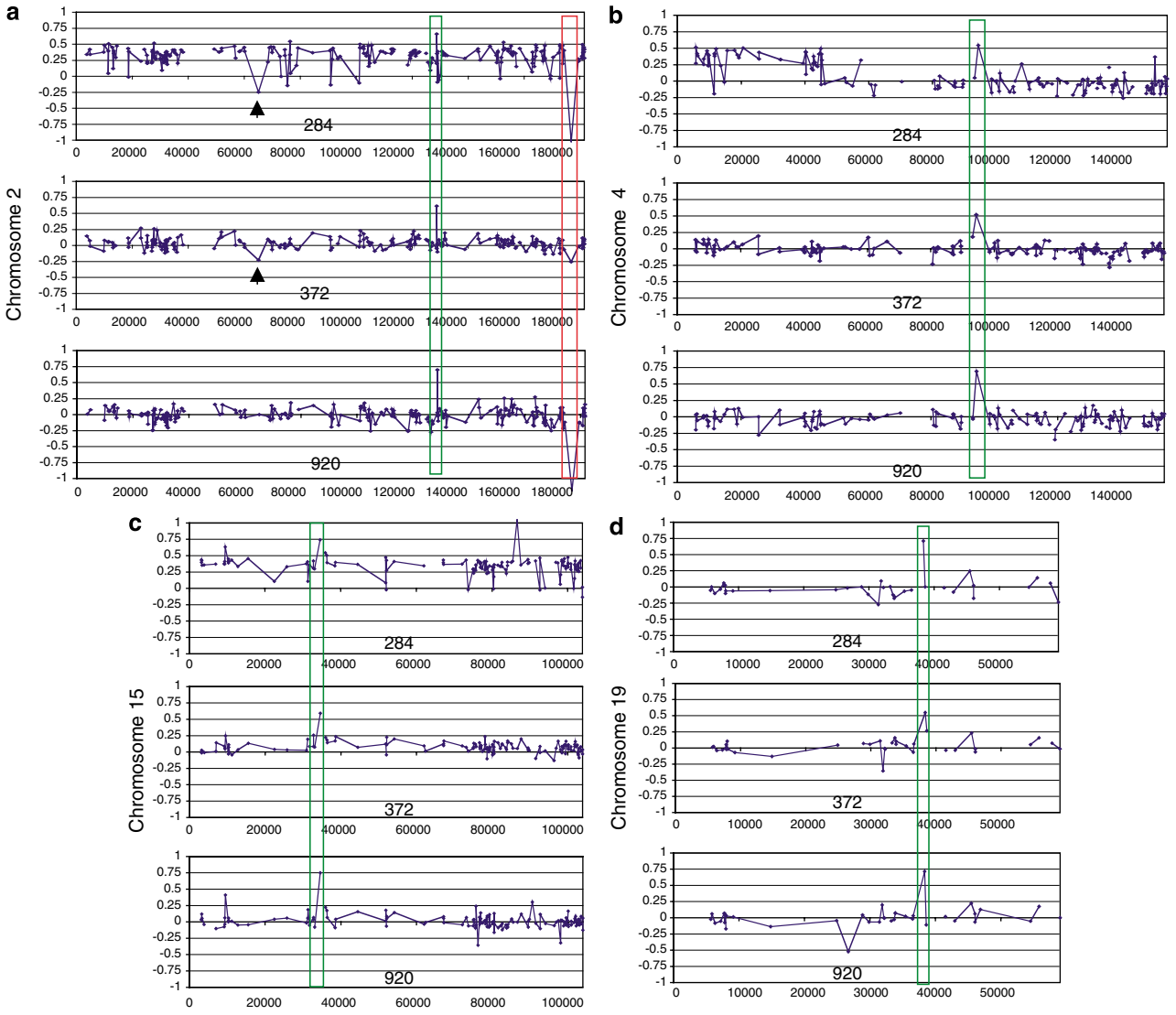

Figure 5 Genomic instability of *Brg1*$^{+/-}$ tumors. Results from array CGH experiments comparing DNA from tumors (284, 372 and 920) to DNA from kidneys of the same mice for chromosomes 2 (**a**), 4 (**b**), 15 (**c**) and 19 (**d**). Each panel has chromosomal DNA plotted along the *x* axis from proximal (left) to distal (right) in kilobase. DNA copy-number changes are plotted along the *y* axis on a log 2 scale. Chromosomal segments that have a gain or loss of at least 0.25 in each tumor are enclosed by green and red boxes, respectively. In addition, black arrowheads point to a segment of chromosome 2 that has a loss of at least 0.25 in tumors 284 and 372. It is also evident that tumor 284 has a ~60 Mb gain of proximal chromosome 4 and trisomies of chromosomes 2 and 15.

differences and how they result in seemingly unrelated tumor phenotypes must still be elucidated.

It is also surprising that BRG1 and SNF5 are the only SWI/SNF-related subunits known to protect against cancer *in vivo* considering that several other subunits interact with cancer-related proteins and are not expressed in tumor-derived cell lines. Some of these subunits have been mutated (*Baf155*/*Srg3* and *Baf180*) or perturbed by RNAi (*Baf60c*) and confer embryonic lethality, but heterozygotes or partial knockdown specimen are not predisposed to cancer (Lickert *et al*., 2004; Wang *et al*., 2004). On the one hand, it is possible that not enough of these mice have been monitored for a long enough time for tumors to be detected. On the other hand, it is possible that only a few subunits protect against cancer and do so in different tissues using different strategies for reasons that are currently unclear. It is also possible that BRG1 and SNF5 protect against cancer by functioning outside of canonical SWI/SNF-related complexes. For example, BRG1 and SNF5 are present in other chromatin-modifying complexes such as NCoR, MLL and REST/co-REST (although BAF155 is too).

Brg1 is a new member of a growing list of tumor-suppressor genes that are haploinsufficient instead of undergoing LOH. A total of ~50% gene dosage is not enough to prevent cancer in some *Brg1* heterozygotes, particularly if other chromosomal alterations or mutations occur elsewhere in the genome. In support of this notion, *Brg1*$^{+/-}$ tumors exhibited DNA copy-number

changes, and five chromosomal segments were duplicated/amplified or deleted in each tumor that was analysed. Some of the chromosomal segments that were altered contain candidate genes that might be involved in the initiation or progression of tumorigenesis.

The histopathology and expression profiles of tumors from *Brg1*$^{+/-}$ and *Wap-T121* mice were not as similar as anticipated, and we also did not detect a genetic interaction between the *Brg1*$^{+/-}$ and *Rb*$^{+/-}$ tumor phenotypes. These results are surprising considering the strength of the BRG1–RB connection *in vitro*, but they are consistent with *Snf5*-deficient primary fibroblasts having normal expression of RB-repressed E2F target genes (Klochendler-Yeivin *et al*., 2006). Our results are also consistent with lack of an obvious genetic interaction between *Snf5* and *Rb* with respect to tumor spectrum, penetrance and size in two mouse studies (Isakoff *et al*., 2005; Guidi *et al*., 2006). Therefore, it remains to be determined whether SWI/SNF-related complexes and RB cooperate to prevent cancer *in vivo*.

BRG1 mutations have been reported in human breast cancer cell lines (Muchardt and Yaniv, 2001) but not in primary breast cancer tumors although it is not clear how many primary tumors have been analysed. The results described here suggest *BRG1* should be screened for mutations or epigenetic silencing in primary tumors from breast cancer patients. *BRG1* should also be analysed, because it maps to 19p13.2, which is thought to harbor several tumor-suppressor genes that protect against breast cancer and other cancers (Oesterreich *et al*., 2001; Yang *et al*., 2004).

Materials and methods

Mice and genotyping
Brg1$^{+/-}$ mice were maintained on a mixed genetic background (C57BL/6J, 129/Sv and CD1) and genotyped by PCR as previously described (Bultman *et al*., 2000). *Rb*$^{+/-}$ and *Brm*$^{-/-}$ mice were maintained on C57BL/6J and 129/Sv inbred backgrounds, respectively. They were genotyped by PCR as previously described.

Histology
Tumors were fixed in 4% paraformaldehyde, embedded in paraffin and 5 μm sections were cut according to standard procedures. Sections were either stained with H&E or processed for immunofluorescence or *in situ* hybridization as described below.

Gene-expression profiling and data analysis
Total RNA was extracted from tumors using Trizol reagent (Invitrogen, Carlsbad, CA, USA) and integrity was assessed using the RNA 6000 Nano-LabChip kit followed by analysis using a Bioanalyzer (Agilent, Palo Alto, CA, USA). Tumor and reference samples were cohybridized overnight to Agilent Mouse Oligo Microarrays (G4121A), washed, scanned on an Axon GenePix 4000B scanner, analysed using GenePix 4.1 software and uploaded into our database where a Lowess normalization was automatically performed as previously described (Herschkowitz *et al*., 2007). Data analysis was performed using statistical analysis of microarrays and a false-discovery rate of 1% (Herschkowitz *et al*., 2007).

Immunofluorescence
Paraffin-embedded sections were processed using standard immunostaining methods. The antibodies and their dilutions were cytokeratin 5 (K5, 1:8000, Covance, PRB-160P), cytokeratin 14 (1:1000, Covance, PRP-155P) and cytokeratins 8/18 (K8/18, 1:450, Progen, GP11). Secondary antibodies were conjugated to Alexa-488 or -594 fluorophores (1:200, Molecular Probes, Invitrogen).

Western blots
Western blots utilized a BRG1 mouse monoclonal antibody that does not cross react with BRM (Santa Cruz, Santa Cruz, CA, USA, G-7) and a β-actin goat polyclonal antibody (Santa Cruz), and were detected using secondary antibodies conjugated to horseradish peroxidase.

In situ *hybridization*
An $\sim$1.4 kb segment of the *Brg1* 3′ untranslated region was amplified by RT–PCR using a 5′-tgtggatcagaaggtgatccaggca-3′ forward primer and a 5′-ccggcacgcgcatgcatcca-3′ reverse primer. The RT–PCR product was subcloned into pGEM-T Easy (Promega, Madison, WI, USA), and plasmid DNA subclones were purified (Promega) that had the insert in each orientation as determined by *Sma*I digestion. Plasmid DNA was linearized with *Sac*II, and antisense and sense riboprobes were synthesized by incorporating digoxigenin-UTP (Roche, Basel, Switzerland) using SP6 and T7 RNA polymerases (Roche), respectively. Hybridization and washing steps were performed following standard procedures. Visualization of the riboprobes was detected using anti-digoxigenin conjugated to alkaline phosphatase and NBT/BCIP according to the manufacturer's protocol.

Array CGH
Array CGH was performed at University of California-San Francisco microarray core facility. The mouse tiling arrays contained 2896 BACs spotted in triplicate with an average spacing of 1 Mb throughout the mouse genome. Hybridizations, imaging, calculation of log2 ratios for integrated Cy3 and Cy5 intensities and statistical analyses were performed as previously described (Snijders *et al*., 2005).

Acknowledgements

This work was supported, in part, by a grant from the NIH.

References

Bultman S, Gebuhr T, Yee D, La Mantia C, Nicholson J, Gilliam A *et al*. (2000). A Brg1 null mutation in the mouse reveals functional differences among mammalian SWI/SNF complexes. *Mol Cell* **6**: 1287–1295.

Dauvillier S, Ott MO, Renard JP, Legouy E. (2001). BRM (SNF2alpha) expression is concomitant to the onset of vasculogenesis in early mouse postimplantation development. *Mech Dev* **101**: 221–225.

Doan DN, Veal TM, Yan Z, Wang W, Jones SN, Imbalzano AN. (2004). Loss of the INI1 tumor suppressor does not impair the expression of multiple BRG1-dependent genes or the assembly of SWI/SNF enzymes. *Oncogene* **23**: 3462–3473.

Guidi CJ, Mudhasani R, Hoover K, Koff A, Leav I, Imbalzano AN *et al*. (2006). Functional interaction of the retinoblastoma and ini1/snf5 tumor suppressors in cell growth and pituitary tumorigenesis. *Cancer Res* **66**: 8076–8082.

Herschkowitz JI, Simin K, Weigman VJ, Mikaelian I, Usary J, Hu Z *et al*. (2007). Identification of conserved gene expression features between murine mammary carcinoma models and human breast tumors. *Genome Biol* **8**: R76.

Isakoff MS, Sansam CG, Tamayo P, Subramanian A, Evans JA, Fillmore CM *et al*. (2005). Inactivation of the Snf5 tumor suppressor stimulates cell cycle progression and cooperates with p53 loss in oncogenic transformation. *Proc Natl Acad Sci USA* **102**: 17745–17750.

Klochendler-Yeivin A, Picarsky E, Yaniv M. (2006). Increased DNA damage sensitivity and apoptosis in cells lacking the Snf5/Ini1 subunit of the SWI/SNF chromatin remodeling complex. *Mol Cell Biol* **26**: 2661–2674.

Lickert H, Takeuchi JK, Von Both I, Walls JR, McAuliffe F, Adamson SL *et al*. (2004). Baf60c is essential for function of BAF chromatin remodelling complexes in heart development. *Nature* **432**: 107–112.

Medina PP, Carretero J, Fraga MF, Esteller M, Sidransky D, Sanchez-Cespedes M. (2004). Genetic and epigenetic screening for gene alterations of the chromatin-remodeling factor, SMARCA4/BRG1, in lung tumors. *Genes Chromosomes Cancer* **41**: 170–177.

Muchardt C, Yaniv M. (2001). When the SWI/SNF complex remodels … the cell cycle. *Oncogene* **20**: 3067–3075.

Oesterreich S, Allredl DC, Mohsin SK, Zhang Q, Wong H, Lee AV *et al*. (2001). High rates of loss of heterozygosity on chromosome 19p13 in human breast cancer. *Br J Cancer* **84**: 493–498.

Reisman DN, Sciarrotta J, Wang W, Funkhouser WK, Weissman BE. (2003). Loss of BRG1/BRM in human lung cancer cell lines and primary lung cancers: correlation with poor prognosis. *Cancer Res* **63**: 560–566.

Roberts CW, Orkin SH. (2004). The SWI/SNF complex – chromatin and cancer. *Nat Rev Cancer* **4**: 133–142.

Simin K, Wu H, Lu L, Pinkel D, Albertson D, Cardiff RD *et al*. (2004). pRb inactivation in mammary cells reveals common mechanisms for tumor initiation and progression in divergent epithelia. *PLoS Biol* **2**: E22.

Snijders AM, Nowak NJ, Huey B, Fridlyand J, Law S, Conroy J *et al*. (2005). Mapping segmental and sequence variations among laboratory mice using BAC array CGH. *Genome Res* **15**: 302–311.

Wang Z, Zhai W, Richardson JA, Olson EN, Meneses JJ, Firpo MT *et al*. (2004). Polybromo protein BAF180 functions in mammalian cardiac chamber maturation. *Genes Dev* **18**: 3106–3116.

Yang TL, Su YR, Huang CS, Yu JC, Lo YL, Wu PE *et al*. (2004). High-resolution 19p13.2–13.3 allelotyping of breast carcinomas demonstrates frequent loss of heterozygosity. *Genes Chromosomes Cancer* **41**: 250–256.

Supplementary Information accompanies the paper on the Oncogene website (http://www.nature.com/onc).